Lasing Action due to the Two-Dimensional Quasiperiodicity of Photonic Quasicrystals with a Penrose Lattice

M. Notomi,[1] H. Suzuki,[2] T. Tamamura,[3] and K. Edagawa[4]

[1]*NTT Basic Research Laboratories, NTT Corporation, 3-1 Morinosato-Wakamiya, Atsugi, 243-0198 Japan*
[2]*NTT Photonics Laboratories, NTT Corporation, 3-1 Morinosato-Wakamiya, Atsugi, 243-0198 Japan*
[3]*NTT Electronics, 3-1 Morinosato-Wakamiya, Atsugi, 243-0198 Japan*
[4]*Institute of Industrial Science, University of Tokyo, 4-6-1 Komaba, Tokyo 153-8505, Japan*

(Received 30 April 2003; published 26 March 2004)

We have fabricated photonic quasicrystal lasers with a Penrose lattice that does not possess translational symmetry but has long-range order, and observed coherent lasing action due to the optical feedback from quasiperiodicity, exhibiting a variety of 10-fold-symmetric lasing spot patterns. The lattice constant dependence of lasing frequencies and spot patterns show complicated features very different from photonic crystal/random lasers, and we have quantitatively explained them by considering their reciprocal lattice. Unique diversity of their reciprocal lattice opens up new possibilities for the form of lasers.

DOI: 10.1103/PhysRevLett.92.123906 PACS numbers: 42.70.Qs, 42.25.Bs, 42.55.Ah, 61.44.Br

Lasers conventionally consist of active gain media and external mirrors, but different types of lasers are now attracting much attention. One type uses a photonic crystal [1] as for gain and feedback. With this photonic crystal laser (PCL) [2,3], the standing wave solution of the Bloch waves at the band edge is the feedback source [4]. Another type is the random laser [5,6] in which the Anderson localization [7] is the feedback source. In both cases, lasing occurs without external feedback. Here, we introduce another type of laser without external feedback, the photonic *quasicrystal* laser (PQCL) with a Penrose lattice [8], in which lasing occurs through *quasiperiodicity*.

Photonic crystals are structures that have periodic refractive-index modulation. Their essential feature is the formation of Bloch states as a result of the periodic perturbation from the lattice with translational symmetry. Photonic quasicrystal*s* (PQCs) have neither true periodicity nor translational symmetry but have a quasiperiodicity that exhibits long-range order and orientational symmetry. Although rotational symmetry other than 2-, 3-, 4-, and 6-fold is prohibited for crystals, any order of rotational symmetry is possible in quasicrystals. Quasicrystals were discovered in nature first in an Al-Mn metallic alloy [9], and exhibit a lot of unique electronic properties [10]. Quasicrystals have many features in common with crystals, but many important concepts that relate to crystals (band structure, Bloch theorem, Brillouin zone, etc.) are invalid. Recently, photonic version of quasicrystals are being discussed and studied [11–14] because there are larger degrees of freedom for modifying optical properties than in photonic crystals.

Then, is it possible to obtain lasing without mirror feedback if we introduce gain into PQCs? If so, what type of lasing action is realized? Can PQCLs lase in extended bulk modes similar to PCLs or in localized modes? Can lasing properties such as wavelength, mode profile, and output be controlled by the quasiperiodicity? Finding the answers to these questions has been our motivation. Previous work on PQCs has mainly focused on the formation of photonic band gaps. Lasing modes in PCLs are normally extended modes, and if those in PQCLs are also extended, this work will shed light on another aspect of PQCs not covered by previous studies which discussed localized modes. We believe that the most interesting feature of quasiperiodicity is its coherent long-range order and should appear in delocalized extended modes.

Our PQCL is schematically shown in Fig. 1(a). The fabrication process is similar to that of PCLs we reported before [3] We made a 150-nm-deep quasiperiodic hole pattern of 500-μm square in a 1-μm-thick SiO_2 layer on a Si substrate by *e*-beam lithography and reactive ion etching, and we deposited a 300-nm-thick DCM [4-dicyanmethylene-2-methyl-6-(*p*-dimethylaminostyryl)-4H-pyran]-doped Alq_3 layer on the patterned SiO_2 by coevaporation. The Penrose lattice is realized by filling the 2D space with two types of rhombuses whose edges have the same length (quasilattice constant a). The lattice does not have translational symmetry but has long-range order and 10-fold rotational symmetry. We numerically generated the Penrose lattice by the generalized dual method [15], and formed circular holes at the center of every rhombus. We fabricated a series of 24 samples with $a = 180$–660 nm. Figure 1(b) shows scanning electron micrographs of our patterned samples before deposition.

When the samples were optically pumped by a 0.6-ns pulsed nitrogen laser operating at 337 nm, we observed a clear lasing action above the pumping threshold around 100 nJ/mm^2, comparable to that of PCLs [3]. The lasing wavelength (λ_L) is different for different a, and falls between 600–650 nm, which corresponds to the DCM gain width. We measured emission spectra in the

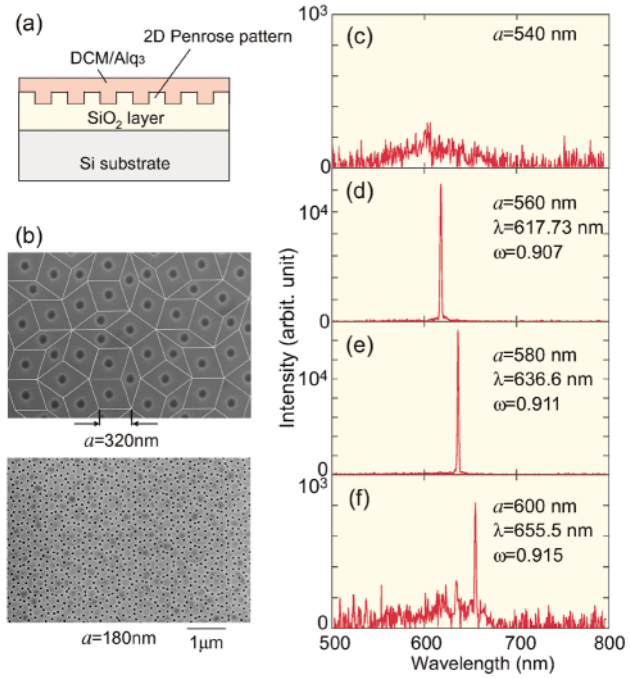

FIG. 1 (color). (a) Schematic view of PQCLs; (b) scanning electron micrographs; (c)–(f) emission spectra of samples with $a = 540$, 560, 580, 600 nm.

perpendicular direction to the sample. Figure 1(c) shows the spectrum of a nonlasing sample that exhibits a broad spontaneous emission. Figures 1(d)–1(f) show spectra for lasing samples in which there are sharp single peaks whose widths are nearly the resolution limit. Note that for these three samples, λ_L almost scales with a. The normalized lasing frequency ω_L ($= n\lambda_L/a$) is almost the same for these three, which indicates that the same gap edge is the origin of the lasing. If we classify all the lasing samples in terms of ω_L, some of the samples exhibit almost the same ω_L but we still observed many different ω_L [see also Fig. 3(b)]. We previously reported similar behavior in PCLs [3], but the number of different ω_L was much less than in the present case.

For lasing samples, we observed several bright spots emitted in the out-of-plane direction. We used a CCD camera to record these spots projected on a screen as shown in Fig. 2(a). The recorded spot images are shown in Figs. 2(b)–2(e). All the spot images exhibit apparent 10-fold rotational symmetry. This symmetry cannot coexist with the translational symmetry. It is worth remembering here that the first report of the Al-Mn quasicrystal was the observation of electron diffraction spots with 10-fold symmetry [16]. Our observation indicates that the lasing action is due to the feedback of the quasiperiodic long-range order. In addition, these spot images are similar for different samples with the same ω_L, but differ when ω_L are different. The observed spot images are well localized and the far-field angle is less than 1°, which is comparable to that of our PCLs. The size of the spots is

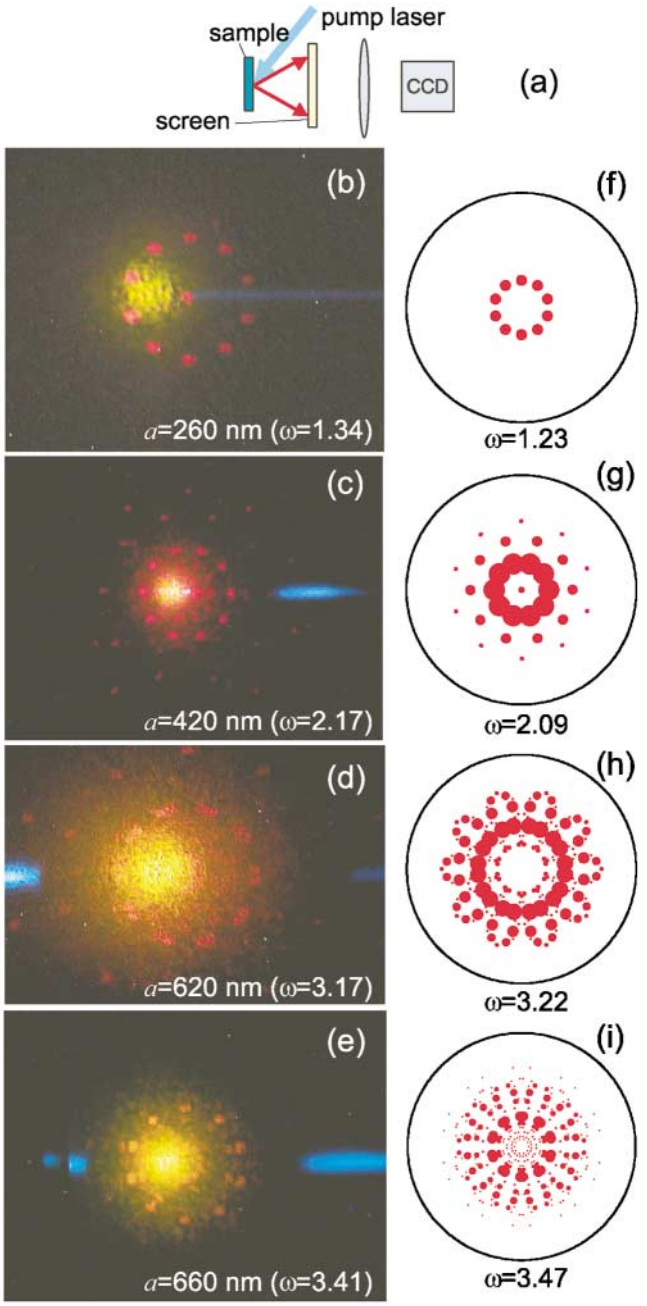

FIG. 2 (color). Spot images of the out-of-plane emission. (a) measurement setup. (b)–(e) measured spot images. (f)–(i) spot images calculated from the reciprocal lattice. See also Fig. 4.

related to localization in k space, and thus to the coherence area of the lasing mode. PCLs with bad homogeneity exhibit diffused streak patterns instead of spot patterns. Therefore, the present result indicates that the lasing action is the result of well-defined extended modes that are coherently spread throughout the sample. A rough estimation indicates that the coherent length is at least larger than $100a$. With this issue, this lasing property is very different from that of random lasers. In a strong

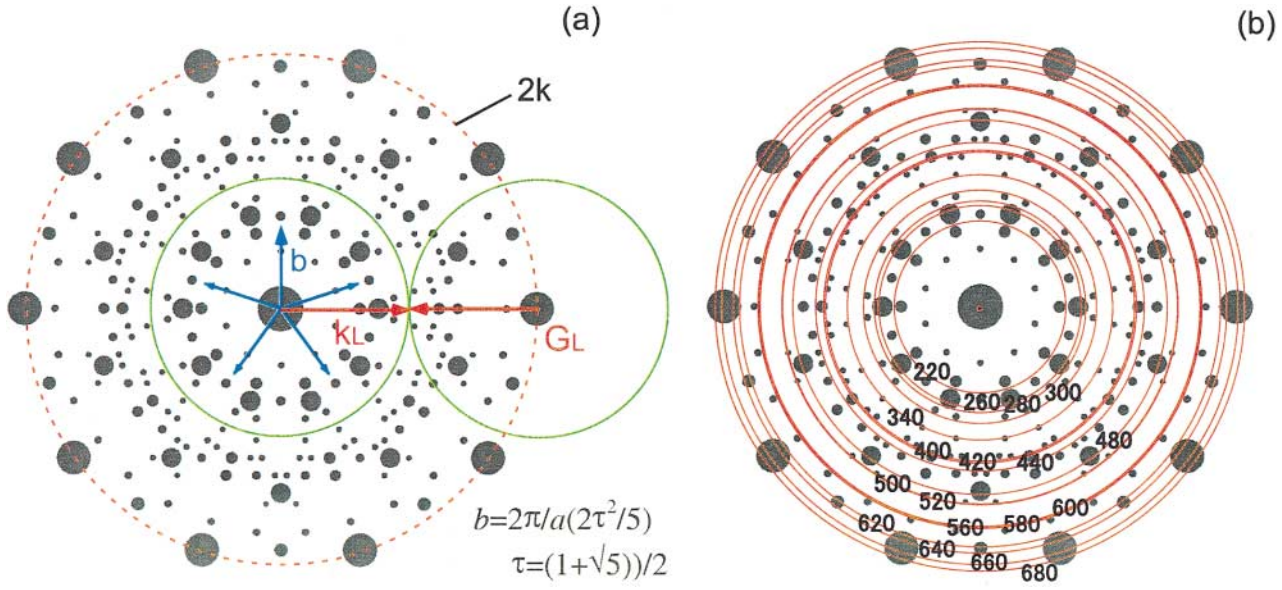

FIG. 3 (color). Reciprocal lattice representation of lasing condition. The diameter of spots is proportional to the Fourier amplitude. (a) An example of lasing condition. (b) $2k$ circles deduced experimentally are overlapped on the reciprocal lattice.

localization regime, their lasing modes are highly localized in real space. In a weak localization regime, they have no definite lasing modes.

From the analogy with PCLs [2,3] it is suggested that λ_L and diffraction spot patterns are determined by standing wave modes. With PCLs, the λ_L and mode profiles for standing waves can be determined by conventional band calculations. We cannot adopt the same approach with PQCLs because the bands cannot be properly defined. Here we show that we can analyze the lasing mode in terms of their reciprocal space. In Fourier space, quasicrystals are expressed as a discrete set of reciprocal lattice points. Figure 3(a) shows a Fourier transformation of the lattice points of our PQCLs, which is a good approximation of the reciprocal lattice of our PQCs. If a wave $\mathbf{k}$ is generated, it will be multiply scattered by the lattice. Such a wave can be expressed as a linear combination of plane waves diffracted by all the reciprocal lattice points. This expression is valid for periodic and quasiperiodic crystals [17,18]. The lasing condition is equivalent to the standing wave condition in the reciprocal space, expressed as $\sum(\mathbf{k} - \mathbf{G}_j) = 0$. With PCLs, symmetry points (e.g., K, M, G in hexagonal crystals) in the first Brillouin zone (BZ) satisfy this condition. With PQCLs, we have to use the full reciprocal space as shown in Fig. 3(a). The simplest two-wave coupling case is $\mathbf{k} + (\mathbf{k} - \mathbf{G}) = 0$, which can be graphically expressed as a circle with a radius of $2k$. If this $2k$ circle intersects a certain point $\mathbf{G}$, then $\mathbf{k} + (\mathbf{k} - \mathbf{G}) = 0$ is satisfied and a standing wave is formed. In Fig. 3(b), we plot $2k$ circles by using the normalized k deduced from the experimentally determined ω_L. Note that most of the $2k$ circles intersect major reciprocal lattice points. This means that the $\mathbf{k} + (\mathbf{k} - \mathbf{G}) = 0$ is satisfied in our lasers. Although the standing wave condition is satisfied only at symmetry points in the first BZ for PCLs, there are a large number of lasing points satisfying the standing wave condition for PQCLs. This is because all reciprocal points outside the first BZ are identical to those inside the first BZ in PCLs, but which is not the case in PQCLs. This explains why we observed many different ω_L.

Next, we analyzed the diffraction spots using the reciprocal lattice of the PQCs. In PCLs, light can be emitted as radiation modes in the out-of-plane direction, if the phase matching condition is satisfied between the lasing modes and the radiation modes in air by obtaining additional $\mathbf{G}$. If the diffraction spots in PQCLs are governed by the same origin, they should be determined by the ω_L and reciprocal lattice points. The phase matching condition is expressed in the reciprocal space as follows: take one of the lasing modes ($\mathbf{G}_L$), and draw a dispersion circle (light cone) of air with a radius $\omega a/c$ (k_0) centered at $\mathbf{G}_L$. If there are major reciprocal lattice points ($\mathbf{G}_c$) within the circle, this lasing mode can be emitted in a direction parallel to $\mathbf{k}_R$ on the dispersion sphere [$\mathbf{k}_R$ is a vector that ($\mathbf{G}_L - \mathbf{G}_c$) is projected onto the dispersion surface of air]. After considering the symmetry, we obtain a spot image of this lasing condition (see inset). Figures 2(f)–2(i) show diffraction spots calculated from the reciprocal lattice points. Comparing Figs. 2(b)–2(e) and 2(f)–2(i), most of the observed spot images are successfully explained by this calculation.

Furthermore, we classify the $2k$ circles and reciprocal lattice points in Fig. 3(b) according to the spot images of the corresponding lasing modes. We show the circles and reciprocal lattice points with different colors for different spot images in Fig. 4(b). For reciprocal lattice points, each color represents a classification of symmetry

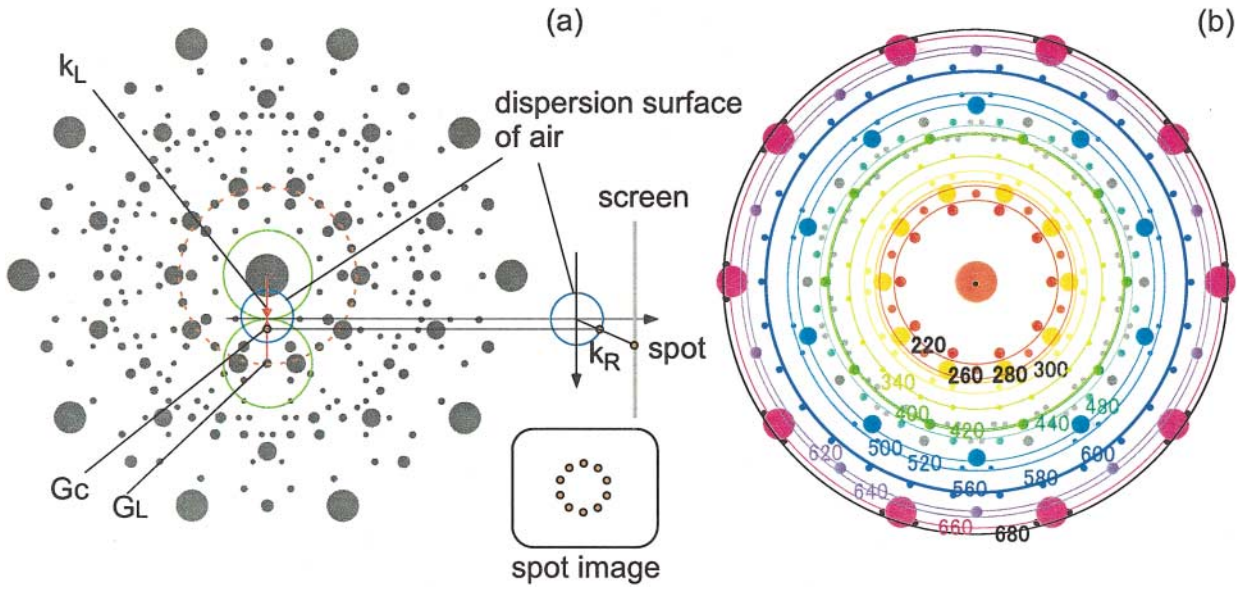

FIG. 4 (color). Reciprocal lattice representation of out-of-plane emission. (a) Lasing condition with G_L induces out-of-plane emission in the k_R direction as a result of diffraction coupling with G_c. (b) $2k$ circles and reciprocal lattice points shown in different colors according to their spot images.

patterns of spot images calculated by the method presented in Fig. 4(a). For circles, the same color set is used for representing the symmetry pattern of observed lasing spots. In most cases, each of the $2k$ circles and the nearest reciprocal lattice point have the same color, which means that they have the same symmetry pattern. The exceptions are colored by gray, which we believe to be explained by multiwave coupling. Therefore, the diffraction spots in Figs. 2(b)–2(e) are explained by diffraction coupling due to the quasiperiodicity in PQCLs, and the results in Figs. 2 and 4(b) clearly show that the $2k$ circle representation presented here largely explains the observed lasing action. It is now clear that the local configuration around the lasing mode $\mathbf{G}_L$ in the reciprocal lattice determines what type of spot images appear. There are a wide variety of spot images because most of the reciprocal lattice points are nonidentical in the PQCs. Finally, we point out that although electron diffraction images in electronic quasicrystals are quite close to the reciprocal lattice itself [16], the diffraction spots of PQCLs are different from the reciprocal lattice. The spot patterns in PQCLs are determined by the local configuration of the reciprocal lattice near the lasing mode $\mathbf{G}_L$.

In summary, we successfully explained the a dependence of λ_L and diffraction spots for PQCLs in terms of their discrete reciprocal lattice representation for extended modes. These results show that lasing action due to standing waves coherently extended among bulk quasicrystals is indeed possible in PQCs that do not have true periodicity or translational symmetry. Considering the wide variety of the reciprocal lattices for quasicrystals, various lasing conditions will be possible. Although the PCL lasing modes are limited by the allowed symmetry for crystals, there is no such limitation in PQCLs. Actually, an arbitrary order of rotational symmetry can be easily generated by the generalized dual method.

[1] J. D. Joannopoulos, P. R. Villeneuve, and S. Fan, Nature (London) **386**, 143 (1997).
[2] S. Noda *et al.*, Science **293**, 1123 (2001).
[3] M. Notomi, H. Suzuki, T. Tamamura, Appl. Phys. Lett. **78**, 1325 (2001).
[4] In fact, a conventional distributed feedback laser can be viewed as a 1D PCL. But in 2 or 3D PCLs, longitudinal and transverse modes are both determined by the photonic band.
[5] N. M. Lawandy *et al.*, Nature (London) **368**, 436 (1994).
[6] H. Cao *et al.*, Phys. Rev. Lett. **82**, 2278 (1999).
[7] D. S. Wiersma *et al.*, Nature (London) **390**, 671 (1997).
[8] R. Penrose, Bull. Inst. Math. Appl., **10**, 266 (1974).
[9] D. Shechtman *et al.*, Phys. Rev. Lett. **53**, 1951 (1984).
[10] D. R. DiVincenzo and P. J. Steindhardt, *Quasicrystals* (World Scientific, Singapore, 1999).
[11] Y. S. Chan, C. T. Chan, and Z. Y. Liu, Phys. Rev. Lett. **80**, 956 (1998).
[12] M. E. Zoorob *et al.*, Nature (London) **404**, 740 (2000).
[13] X. Zhang, Z. Q. Zhang, and C. T. Chan, Phys. Rev. B **63**, R081105 (2001).
[14] M. Bayindir *et al.*, Phys. Rev. B **63**, R161104 (2001).
[15] D. Levine and P. J. Steinhardt, Phys. Rev. B **34**, 596 (1986).
[16] D. Shechtman *et al.*, Phys. Rev. Lett. **53**, 1951 (1984).
[17] A. Y. Kitaev, JETP Lett. **48**, 298 (1989).
[18] P. A. Kalugin *et al.*, Phys. Rev. B **53**, 14 145 (1996).